

New combined control strategy of on-board bidirectional battery chargers for electric vehicles

Khadidja Hadji, Kada Hartani, Tarik Mohammed Chikouche

Electrotechnical Engineering Laboratory, Electrotechnical Department, Faculty of Technology, University of Saida Dr. Moulay Tahar, Saida, Algeria

Article Info

Article history:

Received Feb 20, 2023

Revised May 10, 2023

Accepted May 25, 2023

Keywords:

Battery charger

Electric vehicles

G2V

Power quality

Predictive technique

Unit power factor

V2G

ABSTRACT

This paper aims to develop a bidirectional on-board battery charger for electric vehicles (EVs). The studied battery charger is composed of a bidirectional ac-dc converter as the first stage of conversion and a bidirectional dc-dc converter as the second stage. The first one is controlled by a predictive direct power control strategy based on a space vector modulation technique known as P-SVM-DPC, and the second is used to regulate the battery current and regulate the power direction flow by using a direct current control technique. The choice of its topology has taken into consideration the grid-to-vehicles (G2V) and vehicle-to-grid (V2G) power flow directions. During charging or discharging, the DC/DC converter acts like a buck or boost converter. Using MATLAB/Simulink software, the performance of the battery charger is examined in various operating modes, such as fast charging and quick discharging.

This is an open access article under the [CC BY-SA](https://creativecommons.org/licenses/by-sa/4.0/) license.



Corresponding Author:

Khadidja Hadji

Electrotechnical Engineering Laboratory, Electrotechnical Department, Faculty of Technology

University of Saida Dr. Moulay Tahar

4 P. O. B. 138, 20000 Ennasr, Saida, Algeria

Email: hadji.khadidja@yahoo.com

1. INTRODUCTION

The irreversible transition from vehicles with internal combustion engines (ICE) to electric vehicles with electric motors is caused by the revolutionary contributions of power electronics and such disadvantages of ICE as the emission of greenhouse gases, the quick exhaustion of petroleum, and the rising price of things made from petroleum. Electric vehicles (EVs) has become more attractive over the past few thanks to their advantages that are less noisy, more efficient, and more friendly. What concerns most of those who plan to buy this type of vehicle is the autonomy, how to charge it, the accessibility of many electric recharging stations, and the cost of charging. Currently, there is an advantage in some charging stations, which is that it is possible to replace the empty battery with one that is charged and ready for use power electronic converters are required for EV battery charging, which connects vehicles to the grid using the new technological trends. Each of these trends requires stable power, a bidirectional power converter, and flexible control techniques [1]. The power level of the battery pack determines which AC/DC converter is used for grid-connected devices, like a single-phase half- or full-bridge, a three-phase full-bridge, or a multilevel converter [2], and multilevel topologies such as cascaded H-bridge (CHB), neutral point clamped (NPC), or flying capacitor (FCC) converters are used for high power, reduced voltage, and better output quality [3]. The power supply configuration of an EV must take into account many possible converter topologies. Different converters have different uses, such as increasing efficiency and dependability or having great sensitivity and stability to load variations. It is important to take into account cost of components, techniques for managing hardware

2.1. Bidirectional DC/DC converter circuit analysis

The half-bridge converter is the one who controls the direction of energy through the use of the direct current technique. Depending on whether it is charging or discharging, it functions as a buck converter or a boost converter [21]. The main operation equations can be synthesized for buck and boost modes [22], as follows:

- Buck mode: During this mode, T_{13} and D_{14} are turned *on*. The main equations governing operation in buck mode are as (1) and (2), when T_{13} is turned *on*: $V_{Cbus} > V_{batt}$.

$$\begin{cases} V_L = L \frac{di_L}{dt} = V_{Cbus} - V_{batt} \\ i_L = \frac{1}{L} \int_0^{T_{on}} (V_{Cbus} - V_{batt}) dt \end{cases} \quad (1)$$

When D_{14} is turned *on*

$$\begin{cases} L \frac{di_L}{dt} = -V_{batt} \\ i_L = \frac{1}{L} \int_{T_{on}}^{T_{off}} -V_{batt} dt \end{cases} \quad (2)$$

So:

$$\langle V_{Lbuck} \rangle = D(V_{Cbus} - V_{batt}) - (1 - D)V_{batt} = 0 \Rightarrow V_{batt} = DV_{Cbus} \quad (3)$$

Where:

$$D = \frac{T_{on}}{T_{off}} \quad (4)$$

- Boost mode: During this mode, T_{14} and D_{13} are turned *on*. The main equations governing this mode by (5), when T_{14} is turned *on*: $V_{batt} < V_{Cbus}$.

$$\begin{cases} L \frac{di_L}{dt} = -V_{batt} \\ i_L = \frac{1}{L} \int_{T_{on}}^{T_{off}} -V_{batt} dt \end{cases} \quad (5)$$

When D_{13} is turned on:

$$\begin{cases} L \frac{di_L}{dt} = V_{Cbus} - V_{batt} \\ i_L = \frac{1}{L} \int_{T_{on}}^{T_{off}} (V_{Cbus} - V_{batt}) dt \end{cases} \quad (6)$$

$$\langle V_{Lboost} \rangle = -DV_{batt} + (1 - D)(V_{Cbus} - V_{batt}) = 0 \Rightarrow V_{batt} = (1 - D)V_{Cbus} \quad (7)$$

The ratio relationship between the chopper sides can be controlled using a PWM signal. with the drive T_{on} and cut-off T_{off} timings forming one switching period T . The duty-cycle D of this circuit determines the voltage conversion ratio, which may be described in (3) in the buck scenario and (7) for the boost scenario. while sizing this inductor Taking into account the greater power output when the battery is charged Regardless of the manner of operation, the voltage is lower. In (8) is the result for buck mode:

$$L = \frac{V_{Cbus} - V_{batt}}{2\Delta i_L} T_{on} \quad (8)$$

The (8) is obtained using (3) for the buck mode.

$$\begin{cases} T_{on-min} = \frac{V_{batt-min}}{V_{Cbus}} T \\ T_{on-max} = \frac{V_{batt-max}}{V_{Cbus}} T \end{cases} \quad (9)$$

The (10) is used in the boost mode.

$$L_{boost} = \frac{V_{battnom}}{2\Delta i_L} T_{on} \quad (10)$$

The (11) is obtained using (7) for the boost mode.

$$\begin{cases} T_{onmin} = 1 - \frac{V_{battmax}}{V_{Cbus}} T \\ T_{onmax} = 1 - \frac{V_{battmin}}{V_{Cbus}} T \end{cases} \quad (11)$$

Where: $V_{Cbus} = 500 V$, $V_{battmin} = 330 V$, $V_{battmax} = 385 V$, and $T = 50 \mu s$. The numerical application of in (8), (9), (10) and (11) in brief is shown in Table 1. Using the maximum T_{on} value for the buck case $38 \mu s$ as a result, a $1.2 mH$ chopper inductor is used to verify the smaller size of this charger.

Table 1. Determined parameters for both modes

Mode	T_{onmin}	T_{onmax}	Δi_L	L_{min}	L_{max}	D_{min}	D_{max}
Buck mode	$33 \mu s$	$38.5 \mu s$	2.33	$1.2 mH$	$1.4 mH$	0.66	0.77
Boost mode	$11.5 mH$	$18 mH$	2.33	$0.81 mH$	$1.3 mH$	0.23	0.36

2.2. Shepherd battery model

The EV Battery modeling is subject to the following simplifying assumptions: The amplitude of the current has no impact on the battery's capacity; the temperature has no impact on the model's performance; and the battery's self-discharge is not reflected. As illustrated in Figure 2, the battery model is an internal resistance connected in series to a regulated voltage source. The regulated voltage source was developed by Shepherd [22], [23]. The electrochemical behavior of a battery is as a function of terminal voltage, state of charge (SOC), internal resistance, discharge current, and open circuit voltage.

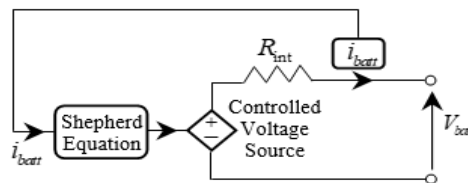


Figure 2. Shepherd battery model

2.3. The discharge model

The proposed discharge model takes into account the open circuit voltage (OCV) as a function of SOC and adds a term describing the polarization voltage and a term concerning the polarization resistance to better represent the OCV behavior [23]. The battery voltage obtained is given by (12).

$$V_{battdisch} = \underbrace{E_0 - V_p}_{V_{ovc}} + \underbrace{A \exp(Bi_{batt}t)}_{V_{exp}} - \underbrace{K \frac{Q}{Q-i_{batt}t}}_{R_p} i_{batt}^* - \underbrace{R_{int} i_{batt}}_{V_{drp}} \quad (12)$$

Where:

$$V_p = K \frac{Q}{Q-i_{batt}t} i_{batt}t$$

K : polarization resistance $\left[\frac{V}{Ah}\right]$, Q : battery capacity $[Ah]$, V_{drp} : ohmique voltage drop $i_{batt}t = \int i_{batt} dt$ actual charge $[Ah]$, A : exponential zone amplitude, R_{int} : internal resistance, B : exponential zone time constant inverse $[Ah]^{-1}$, $[Ω]$, A and B : the exponential zone settings.

2.4. The charge model

The charging behavior varies depending on the type of battery, particularly the end of charge characteristic. In our case, the Li-ion battery charge voltage is the same as in the discharge model, with the exception of the polarization resistance [23], [24]. So, the charge model is given by (13).

$$V_{battch} = \underbrace{E_0 - V_p}_{V_{ovc}} + \underbrace{A \exp(-B i_{batt} t)}_{V_{exp}} - \underbrace{K \frac{Q}{i_{batt} t - 0.1 Q}}_{R_p} i_{batt}^* - \underbrace{R_{int} i_{batt}}_{V_{drp}} \tag{13}$$

2.5. Extracting the parameters and the model validation of the battery

The suggested approach's easy extraction of the dynamic model parameters is a key component. In actuality, obtaining the parameters from the battery does not need doing experimental tests on it. The manufacturer's rating is only three points with the help of MATLAB discharge curve, in steady state, are required to obtain the parameters. In our case, the battery consists of 22 modules connected in parallel to obtain a (330 V, 50 Ah) pack, where each module consists of 100 (3.3 V, 2.3 Ah) cells connected in series. The model validation of the battery pack in MATLAB Simulink gives us these parameters: $E_0 = 357.8385$, $R_{int} = 0.066$, $K = 0.049446$, $A = 27.7121$, $B = 1.2212$. In addition to what is summarized in the Table 2.

Table 2. Simulation and data sheet results of the battery pack

Parameters	Nominal Discharge current	Maximum capacity	Fully charged voltage	End of the exponential zone (Q_{exp} , V_{exp})	Nominal zone (Q_{nom} , V_{nom})	Cut-off voltage	Configuration	Cell number
Value	21.74 A	50 Ah	384.1158 V	(56.5273 Ah, 2.46 V)	(45.22 Ah, 330 V)	247.5 V	247.5 V	2200

3. COMBINED CONTROL DESIGN OF ON-BOARD EV BATTERY CHARGER

3.1. Bidirectional AC/DC converter controller

Figure 3 shows the block diagram of the suggested control a three-phase, three-level NPC rectifier can be controlled using a direct predictive power control (MP-DPC) using a system model to predict the development of system variables through time and deciding on the best controls for the cost function optimization problem, for more detail, please refer to [20], [25], [26].

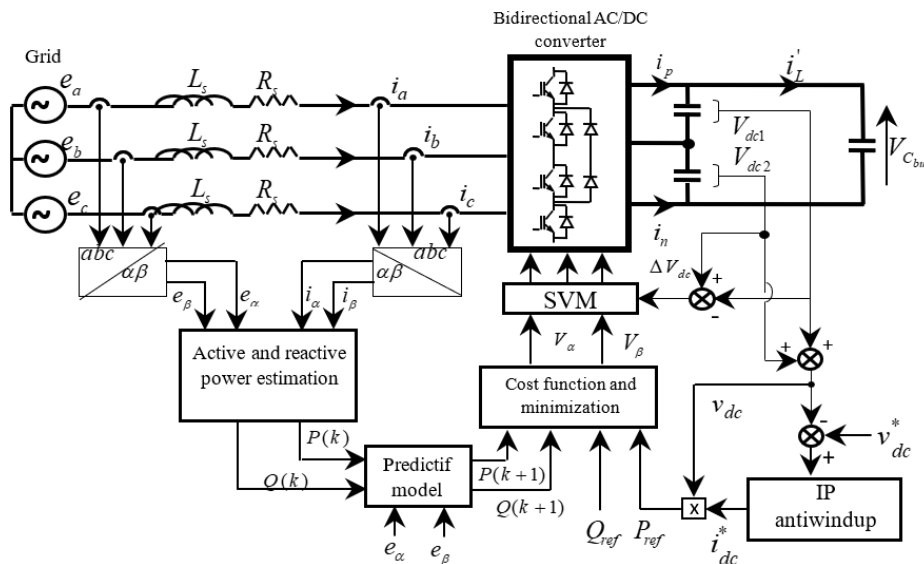


Figure 3. Block diagram of the predictive-DPC of a bidirectional AC/DC converter

3.2. Bidirectional DC/DC converter controller

The direct current technique is employed to regulate the flow of power, operating as buck when T_{13} is triggered (on/off) and a boost converter when T_{14} is triggered. Figure 4 illustrates the DC/DC control design. The difference between reference and measured battery currents determines whether the battery is charging or discharging. This difference travels to the PI controller for tuning the charging or discharging mode. A pulse width modulation (PWM) technique generates pulses from the PI controller's output signal to control of the switches.

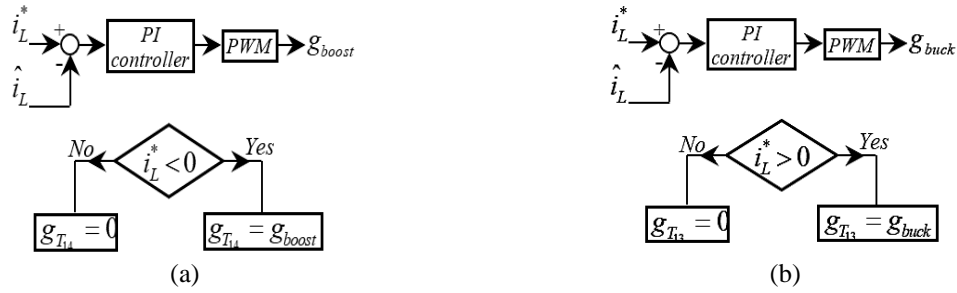


Figure 4. Algorithm of mode selector: (a) discharge and (b) charge

4. SIMULATION RESULTS

Numerical simulations were carried out under the MATLAB/Simulink environment to confirm the robustness of the control structures proposed for the bidirectional on-board battery charger in various operating modes. Numerical simulations were carried out under the MATLAB/Simulink environment to test the robustness of the control structures proposed for the bidirectional on-board battery charger in various operating modes. The electric parameters of the first stage of the charger AC/DC are listed in Table 3.

Table 3. EV Battery charger parameters

	Grid phase voltage	Filter inductance	DC-bus capacitor	DC-bus voltage
AC/DC converter	$V = 70 \text{ V} / f = 50 \text{ Hz}$	$L = 8 \text{ mH}$	$C_{dc} = 5600 \text{ } \mu\text{F}$	$V_{dc} = 500 \text{ V}$

In this simulation test, a reference DC output voltage of 500 V, a reference active power of 5 kW, and a reactive power of 0 VAR are imposed. The initial battery state of charge has been set to 50% in order to confirm that the battery is capable of taking or delivering power as needed. The DC/DC converter controller calculates the reference current required to deliver the required active power shown in Figure 5(a). From this Figure 5, we notice that the power grid follows the computed reference active power. The reactive power is obviously kept at zero in Figure 5(b) to get a unit power factor. According to this figure, predictive DPC control significantly reduces active and reactive power ripples. Figure 5(c) illustrates the voltage tracking waveforms on the DC side. This answer reveals that the DC bus voltage completely matches its reference, as we can see. In actuality, it experiences a small change when the mode is switched at $t = 200 \text{ s}$. A suitable steady-state operation without any static. We notice from Figure 5(d) that the average value of the neutral point voltage is around the zero value.

First, when in G2V operating mode, the battery gets charged from the power grid between 0 and 200 s, and the battery charger draws perfect sinusoidal current from the grid, achieving a unity power factor and enhancing the power quality of the electric power system. The system is configured to charge normally at a current of 50 A, and the battery absorbs around 18 kW of power from the grid. The DC power thus produced can be electrochemically converted and stored in the EV battery. Figure 5(e) shows good tracking of the charging power reference. As shown in Figure 5(f), the battery SOC increased by 5.5% during 200 s (3.33 minutes) to get a more realistic result. Figures 5(g) and 5(h) show the variation of battery current and its terminal voltage. When the battery is charged, we can see that the battery current is constant while the voltage increases almost linearly until it reaches 364 volts.

After $t = 200 \text{ s}$, the V2G mode starts, and the battery's stored energy is returned to the power grid under a current of -50 A and an output power of 18 kW with low current ripple. During this discharging mode, the terminal voltage drops to 346.8 V (Figure 5(h)) and the battery SOC drops by 5.5% (Figure 5(f)), confirming that the DC/DC converter is working properly. Figure 5(i) shows the battery power. Figure 5(j) illustrates the variation of the input current of the DC/DC converter. We notice in V2G mode that the DC/DC converter increases the battery voltage to 853 V to reach the required DC voltage (Figure 5(k)). Figure 5(l) shows that the electrical grid current and voltage are in phase, resulting in a unity of power factor, Figure 5(m). The absorbed currents have a quasi-sinusoidal waveform without ripple in steady state. Figure 5(n) represents the battery discharge stage in the common capacitor between AC/DC and DC/DC converter, meaning it does not absorb current from the electrical grid. The FFT analysis of the grid currents indicates a low rate of harmonic distortion of the absorbed currents (THD = 0.48%), Figure 5(o).

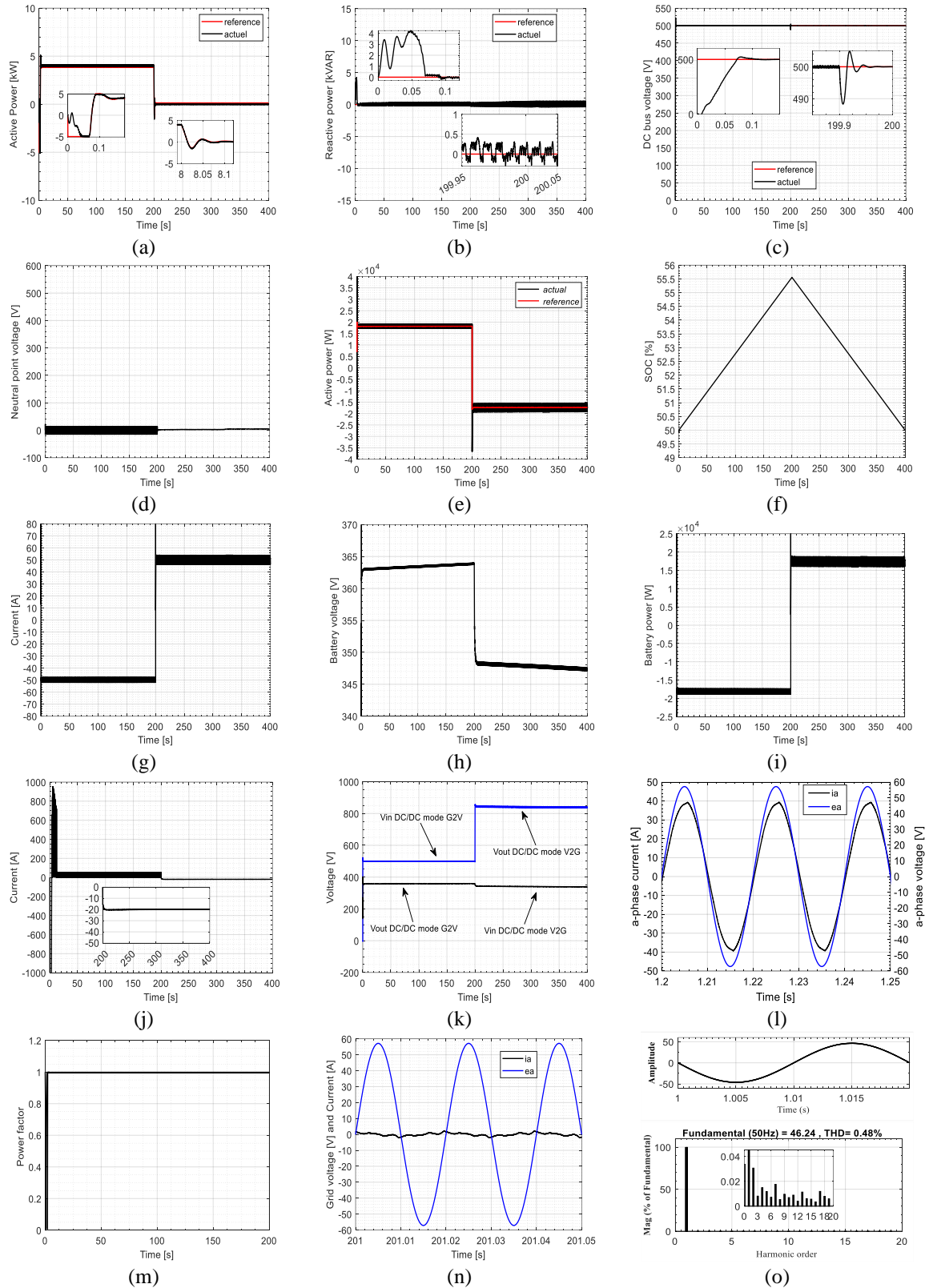


Figure 5. Simulation result: (a) instantaneous active power of grid, (b) instantaneous reactive power of grid, (c) DC bus voltage, (d) neutral point voltage, (e) power of the battery charger, (f) battery SOC, (g) battery current, (h) battery voltage, (i) battery power, (j) load current of the DC/DC converter, (k) DC voltage in G2V and V2G modes, (l) grid voltage and current during G2V mode, (m) power factor, (n) grid current and voltage during V2G mode, and (o) waveform and spectrum of power source current in G2V mode

5. CONCLUSION

Taking the two power flows G2V and V2G into account, a new topology for the on-board EV battery charger is presented in this paper. That allows controlling the instantaneous active and reactive power exchanged between the grid and the EV battery using a combined control based on predictive DPC and direct current control. Simulation results show that the proposed combined control can improve the characteristics of the on-board bidirectional battery charger for electric vehicles in terms of active power regulation in the grid by EV batteries through G2V and V2G modes, unit power factor, low harmonic distortion of grid-injected current, and good dynamic performance of DC-bus voltage stability. This work directs us towards several research perspectives, such as the implementation of the combined control to validate the simulation results under balanced and unbalanced power exchange conditions and the study of other types of bidirectional AC/DC and DC/DC converter structures.

REFERENCES

- [1] A. Saadaoui, M. Ouassaid, and M. Maaroufi, "Overview of Integration of Power Electronic Topologies and Advanced Control Techniques of Ultra-Fast EV Charging Stations in Standalone Microgrids," *Energies*, vol. 16, no. 3, p. 1031, Jan. 2023, doi: 10.3390/en16031031.
- [2] B.-K. Lee, J.-Y. Lee, and D.-H. Kang, "An Isolated PFC Converter with Harmonic Modulation Technique for EV Chargers," in *2018 International Power Electronics Conference (IPEC-Niigata 2018 -ECCE Asia)*, May 2018, pp. 3030–3033. doi: 10.23919/IPEC.2018.8507501.
- [3] J. Zhang, S. Xu, Z. Din, and X. Hu, "Hybrid Multilevel Converters: Topologies, Evolutions and Verifications," *Energies*, vol. 12, no. 4, p. 615, Feb. 2019, doi: 10.3390/en12040615.
- [4] M. Nicholas and D. Hall, "Lessons learned on early electric vehicle fast-charging deployments," *ICCT White Paper*, no. July, p. 54, 2018.
- [5] J. Yuan, L. Dorn-Gomba, A. D. Callegaro, J. Reimers, and A. Emadi, "A Review of Bidirectional On-Board Chargers for Electric Vehicles," *IEEE Access*, vol. 9, pp. 51501–51518, 2021, doi: 10.1109/ACCESS.2021.3069448.
- [6] S. Jaman, S. Chakraborty, D.-D. Tran, T. Geury, M. El Baghdadi, and O. Hegazy, "Review on Integrated On-Board Charger-Traction Systems: V2G Topologies, Control Approaches, Standards and Power Density State-of-the-Art for Electric Vehicle," *Energies*, vol. 15, no. 15, p. 5376, Jul. 2022, doi: 10.3390/en15155376.
- [7] V. Monteiro, J. A. Afonso, and J. L. Afonso, "Bidirectional Power Converters for EV Battery Chargers," *Energies*, vol. 16, no. 4, p. 1694, Feb. 2023, doi: 10.3390/en16041694.
- [8] A. Jain, K. K. Gupta, S. K. Jain, P. Bhatnagar, and H. Vahedi, "A V2G Enabled Bidirectional Single/Three-Phase EV Charging Interface Using Modular Multilevel Buck PFC Rectifier," *Electronics*, vol. 11, no. 12, p. 1891, Jun. 2022, doi: 10.3390/electronics11121891.
- [9] J. Lara, L. Masisi, C. Hernandez, M. A. Arjona, and A. Chandra, "Novel Five-Level ANPC Bidirectional Converter for Power Quality Enhancement during G2V/V2G Operation of Cascaded EV Charger," *Energies*, vol. 14, no. 9, p. 2650, May 2021, doi: 10.3390/en14092650.
- [10] L. Jorge, H. Concepcion, M. A. Arjona, M. Lesedi, and C. Ambrish, "Performance Evaluation of an Active Neutral-Point-Clamped Multilevel Converter for Active Filtering in G2V-V2G and V2H Applications," *IEEE Access*, vol. 10, pp. 41607–41621, 2022, doi: 10.1109/ACCESS.2022.3167694.
- [11] Y. Lu, H. Ma, Y. Wei, Y. Pan, X. Chen, and Y. Huang, "Research on Five-Level PFC Circuit Topology Based on Switch-Diode-Capacitor Network," *Electronics*, vol. 12, no. 6, p. 1286, Mar. 2023, doi: 10.3390/electronics12061286.
- [12] S. Chakraborty, H.-N. Vu, M. M. Hasan, D.-D. Tran, M. El Baghdadi, and O. Hegazy, "DC-DC Converter Topologies for Electric Vehicles, Plug-in Hybrid Electric Vehicles and Fast Charging Stations: State of the Art and Future Trends," *Energies*, vol. 12, no. 8, p. 1569, Apr. 2019, doi: 10.3390/en12081569.
- [13] H. He, R. Xiong, and J. Fan, "Evaluation of Lithium-Ion Battery Equivalent Circuit Models for State of Charge Estimation by an Experimental Approach," *Energies*, vol. 4, no. 4, pp. 582–598, Mar. 2011, doi: 10.3390/en4040582.
- [14] M. Y. Metwly, M. S. Abdel-Majeed, A. S. Abdel-Khalik, R. A. Hamdy, M. S. Hamad, and S. Ahmed, "A Review of Integrated On-Board EV Battery Chargers: Advanced Topologies, Recent Developments and Optimal Selection of FSCW Slot/Pole Combination," *IEEE Access*, vol. 8, pp. 85216–85242, 2020, doi: 10.1109/ACCESS.2020.2992741.
- [15] S. Semsar, T. Soong, and P. W. Lehn, "On-Board Single-Phase Integrated Electric Vehicle Charger With V2G Functionality," *IEEE Transactions on Power Electronics*, vol. 35, no. 11, pp. 12072–12084, Nov. 2020, doi: 10.1109/TPEL.2020.2982326.
- [16] F. Un-Noor, S. Padmanaban, L. Mihet-Popa, M. Mollah, and E. Hossain, "A Comprehensive Study of Key Electric Vehicle (EV) Components, Technologies, Challenges, Impacts, and Future Direction of Development," *Energies*, vol. 10, no. 8, p. 1217, Aug. 2017, doi: 10.3390/en10081217.
- [17] B.-K. Lee, J.-P. Kim, S.-G. Kim, and J.-Y. Lee, "An Isolated/Bidirectional PWM Resonant Converter for V2G(H) EV On-Board Charger," *IEEE Transactions on Vehicular Technology*, vol. 66, no. 9, pp. 7741–7750, Sep. 2017, doi: 10.1109/TVT.2017.2678532.
- [18] A. Phimpui and U. Supatti, "V2G and G2V Using Interleaved Converter for a Single-Phase Onboard Bidirectional Charger," in *2019 IEEE Transportation Electrification Conference and Expo, Asia-Pacific (ITEC Asia-Pacific)*, May 2019, pp. 1–5. doi: 10.1109/ITEC-AP.2019.8903662.
- [19] K. Fahem, D. E. Chariag, and L. Sbita, "On-board bidirectional battery chargers topologies for plug-in hybrid electric vehicles," in *2017 International Conference on Green Energy Conversion Systems (GECS)*, Mar. 2017, pp. 1–6. doi: 10.1109/GECS.2017.8066189.
- [20] K. Hadji, K. Hartani, T. M. Chikouche, and A. E. Ameer, "Predictive Direct Power Control of a Three-Phase Three-Level NPC PWM Rectifier based on Space Vector Modulation," in *2021 12th International Symposium on Advanced Topics in Electrical Engineering (ATEE)*, Mar. 2021, pp. 1–9. doi: 10.1109/ATEE52255.2021.9425052.
- [21] H. N. de Melo, J. P. F. Trovao, P. G. Pereirinha, H. M. Jorge, and C. H. Antunes, "A Controllable Bidirectional Battery Charger for Electric Vehicles with Vehicle-to-Grid Capability," *IEEE Transactions on Vehicular Technology*, vol. 67, no. 1, pp. 114–123, Jan. 2018, doi: 10.1109/TVT.2017.2774189.

- [22] K. M. Tan, V. K. Ramachandaramurthy, and J. Y. Yong, "Bidirectional battery charger for electric vehicle," in *2014 IEEE Innovative Smart Grid Technologies - Asia (ISGT ASIA)*, May 2014, pp. 406–411. doi: 10.1109/ISGT-Asia.2014.6873826.
- [23] O. Tremblay and L.-A. Dessaint, "Experimental Validation of a Battery Dynamic Model for EV Applications," *World Electric Vehicle Journal*, vol. 3, no. 2, pp. 289–298, Jun. 2009, doi: 10.3390/wevj3020289.
- [24] M. Chen and G. A. Rincon-Mora, "Accurate electrical battery model capable of predicting runtime and I-V performance," *IEEE Transactions on Energy Conversion*, vol. 21, no. 2, pp. 504–511, Jun. 2006, doi: 10.1109/TEC.2006.874229.
- [25] T. M. Chikouche, K. Hartani, and T. Terras, "Predictive-DPC Based on Duty Cycle Control of PWM Rectifier under Unbalanced Network," *Periodica Polytechnica Electrical Engineering and Computer Science*, vol. 66, no. 2, pp. 139–147, May 2022, doi: 10.3311/PPee.20048.
- [26] S. S. H. Khadidja, "Commande directe de puissance d'un redresseur MLI triphasé de structure NPC à trois niveaux," Project Master LMD, Département d'Electrotechnique, Faculté de Technologie, Université de Saida, 2018-2019.

BIOGRAPHIES OF AUTHORS



Khadidja Hadji     is Ph.D. student in the Department of Electrotechnics Engineering at the university Dr Moulay Tahar of Saida, Algeria. she was born in Saida, Algeria in 1996, she received B.S. degree in Electro-technical engineering in 2017 and Master degree in Industrial electrical engineering in 2019. His main research interests revolve around power electronics concerning battery charger for electric vehicle. She can be contacted at email: Khadidja.hadji@univ-saida.dz or Hadji.khadidja@yahoo.com.



Kada Hartani     is a lecturer in Electrical & Engineering Department at the University of Saida, Algeria since 2003. He was born in Saida, Algeria in 1976. He obtained his Doctorate in Electrical Control from the University of Sciences and Technology (USTO), Oran, Algeria, in 2007; M.S. in electrical control from the University of Sciences and Technology (USTO), Oran, Algeria, 2003; B.S. in Electrotechnical Engineering from the University of Saida, Algeria, in 1997. Currently, he is a professor in electrical control and director of Electrotechnical Engineering Laboratory at the University of Saida, Algeria. His fields of interest include multi-machine multi-converter systems, antilock brake system, traction control system, and anti-skid control for electric vehicle. He can be contacted at email: kada_hartani@yahoo.fr.



Tarik Mohammed Chikouche     was born in Saida, Algeria, in 1966. He received the B.S. degree in Electrical Engineering from Mohamed Boudiaf University of Sciences and Technologie, Oran, Algeria, in 1991 and the M.S. degree from High National Schools of Technical Studies in 2004. Subsequently, he received the Ph.D. degree from Djillali Liabes University, Sidi Bel Abbès, Algeria, in 2013 and the university habilitation from Doctor Tahar Moulay University of Saida, Algeria in 2018., Algeria. His research interests include electrical machines and drives, energy quality, control of three phase PWM rectifier, and renewable energy. He can be contacted at email: tchikouche@yahoo.fr.